

# Temperature dependent electron–phonon coupling and heat capacity in thin slabs of topological insulator $\text{Bi}_2\text{Te}_3$ as pertinent to the thermal spike model



Paramita Patra\*, S.K. Srivastava

Department of Physics, Indian Institute of Technology Kharagpur, Kharagpur 721302, India

## ARTICLE INFO

### Article history:

Received 11 November 2015  
Received in revised form 18 January 2016  
Accepted 26 January 2016  
Available online 8 February 2016

### Keywords:

Thermal spike model  
Electron phonon coupling  
Density functional theory  
Topological insulator

## ABSTRACT

Electron–phonon coupling strength and electronic heat capacity are essential ingredients of the widely accepted thermal spike model of swift heavy ion matter interaction. The concept, although applicable very well in metals, loses its validity in materials with a band gap, wherein it is customary to take the two quantities merely as adjustable parameters to fit the experimental results. Topological insulators, like  $\text{Bi}_2\text{Te}_3$ , are quite interesting in this regard because they are also metallic albeit near the surface. In this work, we compute by *first-principles* the electron density of states of  $\sim 16$  Å thick  $\text{Bi}_2\text{Te}_3$  slabs of different orientations and demonstrate an unusually high metallicity for the [001] slab. The density of states is then used to calculate the electron–phonon coupling strength and electronic heat capacity as a function of electron temperature. Strongly electron temperature dependent but weak electron–phonon coupling has been observed, along with systematic deviations of the electronic heat capacity from the linear free-electron metal values.

© 2016 Elsevier B.V. All rights reserved.

## 1. Introduction

It is more or less established by now that the mechanism described by the thermal spike model (TSM) [1] of swift heavy ion (SHI) – matter interaction is responsible for almost all observed SHI induced phenomena including SHI mixing [2], electronic sputtering [3], nanostructure synthesis [4], and nano-dimensional phase separation [5]. The TSM is based on a two-temperature model of heat diffusion and is governed mathematically by the following two coupled partial differential equations governing the heat diffusion into the electron and lattice subsystems of the material [1,6]:

$$C_e(T_e) \frac{\partial T_e}{\partial t} = \nabla(K_e(T_e)\nabla T_e) - G(T_e)(T_e - T) + A_e(r, t) \quad (1)$$

and

$$C(T) \frac{\partial T}{\partial t} = \nabla(K(T)\nabla T) + G(T_e)(T_e - T) \quad (2)$$

where  $T_e$ ,  $C_e$ ,  $K_e$ ,  $T$ ,  $C$ , and  $K$  are the temperature, heat capacity, and thermal conductivity of electronic (denoted by the subscript  $e$ ) and lattice subsystems, respectively. Further,  $A_e(r, t)$  is the energy

density per unit time supplied by the incident ions to the electron subsystem at a radial distance  $r$  from the ion path at a time  $t$ , and  $G(T_e)$  is the electron temperature dependent electron–phonon coupling (EPC) strength.

In a typical SHI-matter interaction, the two equations suggest the attainment of several thousands of Kelvins of electron temperature in a sub-picosecond time after the passage of the ion [1,2]. This electronic heat is subsequently transferred to the lattice through the EPC and lattice temperatures exceeding the melting temperature are attainable for an ultra-short (a few  $ps$ ) duration within a cylinder of a few  $nm$  radius around the ion path [1,2], the so-called latent track. Most of the SHI induced processes are assumed to take place, and also proved indirectly so, in this molten state of the latent track [2].

The TSM description, however, is intrinsically valid only in the case of metals, wherein there is a sea of conduction electrons which can devour the energy transferable by the ions. The EPC's,  $K_e$ 's and  $C_e$ 's are theoretically defined for metals and can be used in the above equations to estimate the space and time dependent electron and lattice temperatures. In case of insulators and semiconductors, however, these quantities are not defined. Qualitatively also, there are no mobile electrons in these materials to carry away the transferred ion energy. So, the TSM as such cannot be applied to materials with band gap. Nevertheless, the model

\* Corresponding author.

E-mail address: [patro.paro@phy.iitkgp.ernet.in](mailto:patro.paro@phy.iitkgp.ernet.in) (P. Patra).

is used to explain SHI induced phenomena in band-gapped materials as well by taking the three quantities as adjustable parameters to fit the experimental data [7].

Topological insulators (TIs), which have a full insulating gap in the bulk and metallicity in the surface states and are a new phase of theoretical research attraction [8], would be quite relevant vis-à-vis the application of the TSM. It would be very interesting to see how, with a change in the surface metallicity, the TSM predicted SHI effects compare with the corresponding experimental results. The present work, however, is limited to theoretical estimations of EPC and  $C_e$  (in a TI, viz.  $\text{Bi}_2\text{Te}_3$ ), which are suggested to be put in the TSM for further studies.  $K_e$  is derivable from  $C_e$  via the Wiedemann–Franz law if the electrical conductivity  $\sigma$  is known. As concerns finding the value of  $\sigma$ , first, it is required only when Eqs. (1) and (2) need to be solved for calculating the temperature evolution, and second, its experimental values can be found, e.g., in Ref. [9].

Hitherto, the TSM model calculations of lattice temperature evolution after the passage of SHI have been performed by using the EPC and  $C_e$  determined from the free electron theory of metals [1], which describes only a few noble elemental metals [10] and takes the density of electron states (eDOS) right at the Fermi energy as the sole parameter. A few of the SHI mixing experiments [11] have hinted about the possible contribution of localized  $d$ -electrons as well in the final results. The consideration of the full range of the eDOS, therefore, is mandatory to determine the EPC and  $C_e$ , considering also the ultra-high non-zero Kelvin temperatures attainable by the electrons and the electron temperature dependences of the two quantities. Lin et al. [6] have recently adopted finer definitions of EPC and  $C_e$  to address this issue.

In the present work, we calculate the electron temperature dependent EPC strength and  $C_e$  for  $\text{Bi}_2\text{Te}_3$  surface slabs of width  $\sim 16$  Å for three different orientations – [001], [110] and [111] – of the slabs, first by computing the eDOS's using density functional theory (DFT) and subsequently by adopting Lin et al.'s scheme of EPC and  $C_e$  determination.

## 2. Computational details

The eDOS's were computed using the full-potential linearized augmented plane wave (FLAPW) method of DFT as implemented in the code Wien2K [12]. The Purdue–Burke–Ernzerhof scheme of the generalized gradient approximation was used for the exchange correlation potential [13]. First, the eDOS calculation for bulk  $\text{Bi}_2\text{Te}_3$  was performed in order to compare the results with the literature and thus establish the suitability of the method for further calculations of the eDOS's of the slabs.  $\text{Bi}_2\text{Te}_3$  has rhombohedral structure with space group number 166 ( $R\bar{3}m$ ), lattice parameters  $a = b = 4.463$  Å,  $c = 31.04$  Å,  $\alpha = \beta = 90^\circ$ ,  $\gamma = 120^\circ$ , and five atoms per unit cell [14]. There are three non-equivalent atomic sites: Bi (0.4, 0.4, 0.4), Te1 (0, 0, 0) and Te2 (0.212, 0.212, 0.212). The atoms are arranged in layers in the order Te2–Bi–Te1–Bi–Te2, the sequence being known as a quintuple layer (QL) [15,16]. The QL's are repeated along the  $c$  axis. The structure is shown in Fig. 1. The display of the structure was accomplished by the software XCrySDen [17]. The slabs along [001], [110] and [111] plane, each of width  $\sim 16$  Å, were constructed using the 'structeditor' package of Wien2K [12]. For the computations, the muffin-tin radii  $R_{\text{MT}}$  around both Bi and Te atoms were taken as 2.5 au. The multipolarity within the muffin-tin spheres was restricted to a maximum of  $l_{\text{max}} = 10$ . The wavevector cut-off for the plane waves in the interstitial region was taken as a cut-off of  $k_{\text{max}} = 7.0/R_{\text{MT},\text{min}}$ . The charge density was Fourier expanded up to  $G_{\text{max}} = 14 \sqrt{R_{\text{y}}}$ .

For the calculations of  $G(T_e)$  and  $C_e(T_e)$ , the equations used by Lin et al. [6], which take into consideration the whole range of

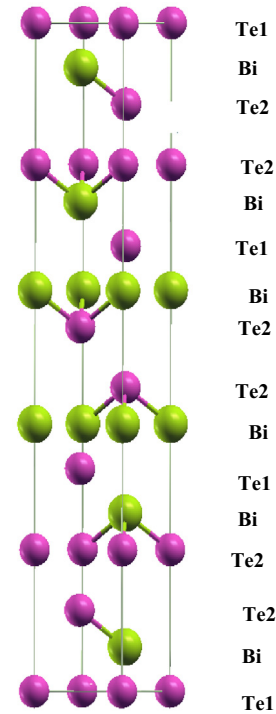


Fig. 1. The unit cell of  $\text{Bi}_2\text{Te}_3$ . The layers are labeled on the right side.

exact eDOS, have straightforwardly been adopted. The equations are:

$$G(T_e) = \frac{\pi \hbar k_B \lambda < \omega^2 >}{g(\varepsilon_F)} \int_{-\infty}^{\infty} g^2(\varepsilon) \left[ -\frac{\partial f(\varepsilon, T_e)}{\partial \varepsilon} \right] d\varepsilon \quad (3)$$

and

$$C_e(T_e) = \int_{-\infty}^{\infty} g(\varepsilon) \left[ -\frac{\partial f(\varepsilon, T_e)}{\partial T_e} \right] \varepsilon d\varepsilon \quad (4)$$

Here,  $g(\varepsilon)$  is the energy dependent eDOS,  $\varepsilon_F$ , the Fermi energy ( $E_F$ ),  $f(\varepsilon, T_e)$ , the Fermi–Dirac distribution function given by  $f(\varepsilon, T_e) = 1 / \{1 + \exp[(\varepsilon - \varepsilon_F) / k_B T_e]\}$ ,  $\lambda$ , the electron band mass enhancement parameter, and  $< \omega^2 >$  is the second moment of the phonon spectrum. Numerical integrations of the two equations were performed by using the DFT generated eDOS's as  $g(\varepsilon)$  and taking the slab value of  $\lambda (= 0.05)$  from Ref. [18]. For  $< \omega^2 >$ , the suggestion  $< \omega^2 > \approx \theta_D^2 / 2$  in Ref. [6], where  $\theta_D$  is the Debye temperature, was followed, and  $\theta_D = 155$  K was taken from Ref. [19].

## 3. Results and discussions

Fig. 2 shows total eDOS's of the bulk  $\text{Bi}_2\text{Te}_3$  and of the three slabs. The bulk  $\text{Bi}_2\text{Te}_3$ , according to the figure, displays a band gap of 0.59 eV, which, apart from its shape, is in good agreement with the earlier computational report by Xiong et al. [20]. This establishes the reliability of the present computational method for the TI. Obviously,  $G(T_e)$  cannot be calculated for this insulator because the Eq. (3) is invalid in this case. This way, computing  $C_e(T_e)$  for the bulk  $\text{Bi}_2\text{Te}_3$  is irrelevant because in the absence of  $G(T_e)$  Eqs. (1) and (2) cannot be solved. In the present work, therefore, we do not attempt to calculate  $G(T_e)$  also. Further the eDOS of [111] slab is also in accordance with the literature [21] with a finite eDOS at  $E_F$  with a smaller band gap beyond the  $E_F$ . This feature displays a weak metallicity for the slab. The eDOS of the [110] slab is slightly different from that of the [111] slab,

Download English Version:

<https://daneshyari.com/en/article/1679717>

Download Persian Version:

<https://daneshyari.com/article/1679717>

[Daneshyari.com](https://daneshyari.com)